Large Interlayer Relaxation at a Metal-Oxide Interface: The Case of a Supported Ultrathin Alumina Film

Erik Vesselli,[1,2] Alessandro Baraldi,[1,2,*] Silvano Lizzit,[3] and Giovanni Comelli[1,2]

[1]*Physics Department and CENMAT, University of Trieste, Via Valerio 2, I-34127 Trieste, Italy*
[2]*IOM-CNR Laboratorio TASC, Area Science Park, S.S. 14 Km 163.5, I-34149 Trieste, Italy*
[3]*Sincrotrone Trieste S.C.p.A., Area Science Park, S.S. 14 Km 163.5, I-34149 Trieste, Italy*

(Received 7 April 2010; published 21 July 2010)

The structure of the metal-oxide interface in the alumina/$Ni_3Al(111)$ system is investigated by comparing backscattering and forward-scattering photoelectron diffraction modulation functions of chemically nonequivalent aluminum and oxygen species with multiple-scattering simulations. We observe large relaxation effects at the metal-oxide interface layer: Al atoms of the Ni_3Al alloy surface are lifted by more than 0.7 Å above the ideal termination, thus creating a new, metallic layer between the oxide and the alloy. The effect of the interface atomic rearrangement on the properties of the supported ultrathin alumina oxide film is discussed.

DOI: 10.1103/PhysRevLett.105.046102 PACS numbers: 68.47.Jn, 61.05.js, 68.55.J−

The growing interest in ultrathin oxide layers arises from their surprising properties, which are expected to play a central role in the development of new electronic, chemical, and sensing technologies such as lasers, memory devices, fast transistors, and fuel cells [1]. The progress in the comprehension of the oxide layers' growth mechanisms and in the characterization of their properties is accompanied by unexpected recent findings. For example, electrons at the interface of ultrathin films show a very large mobility even though the involved compounds are insulating oxides ($LaAlO_3$ and $SrTiO_3$) [2], while superconductive behavior was reported in bilayers consisting of an insulator (La_2CuO_4) and a metal ($La_{1-x}Sr_xCuO_4$), neither of which is a superconducting material as a standalone [3]. It is clear that a precise structural knowledge of the atomic positions at heterostructure junctions is a prerequisite for the rational design of ultrathin oxide films interfaces with tailored properties for applicative purposes. However, the breaking of the translational symmetry and the abrupt discontinuity often result in a large atomic rearrangement, confined within few Å from the interface, which is difficult to characterize experimentally. Because of the large lattice mismatches, the crystalline periodic structural modifications in general extend laterally over few nanometers, thus strongly limiting the applicability of diffraction-based techniques due to the large dimensions of the unit cells, including up to thousands of atoms.

A relevant class of materials is represented by the ultrathin epitaxial oxide films grown on metal substrates. These systems are largely employed as model catalyst supports, and as templates for active metal cluster deposition [4,5]. The most severe limitation for the direct transferability of experimental results to bulk oxide surfaces consist in neglecting the influence of interface and thickness on the oxide properties. Indeed, recent studies have shown that these systems cannot be considered as simple analogs of the corresponding thicker films [6]. Significant variations in the atomic structure at the interface can result in different electronic properties, such as largely modified work function, electron affinity, and charge transfer capabilities [6,7].

In this contest, ultrathin alumina films are considered of great interest, not only as supports in heterogeneous catalysis, but also for their application in the development of new high-K gate nanocapacitors [8], protective coatings against corrosion, and templates for nanopatterning [9]. It is well known that long-range ordered alumina films can be grown on several Ni_xAl ($x = 1, 3$) alloy low index terminations [9–11]. Similarly to the case of NiAl(110) [10,11], at the $Ni_3Al(111)$ surface the oxide film grows in a nonstoichiometric O-Al-O-Al stacking sequence, with almost coplanar terminal layers (Al_t and O_t) and distorted Al hexagons, pentagons, and triangles at the interface (Al_i), resulting in a $(\sqrt{67} \times \sqrt{67})R12.2°$ periodic structure [9]. After extensive experimental investigations [12–17], only recently was the complex oxide film structure unambiguously determined, using a combination of *ab initio* simulations and scanning tunneling microscopy (STM) experiments [9]. Despite this remarkable result, the morphology of the metal-oxide interface remains largely unsolved because of the insensitivity of the scanning probe techniques to the underlying layers.

In the present work we determine the structure of the interface layer by employing chemical state-specific x-ray photoelectron diffraction (XPD) [18] in both back- and forward-scattering regimes. The possibility to separate chemically nonequivalent atomic species allowed us to unveil a large modification of the interface morphology.

The measurements were carried out at the SuperESCA beam line of Elettra [19], and in a dedicated ultrahigh vacuum chamber [20]. Photon energies in the 150–270 (620–680) eV range were used for collecting Al $2p$ (O $1s$) core

level spectra at low kinetic energy with high energy resolution in order to resolve the chemically shifted components. Conversely, monochromatic Al K_α radiation was used for the forward-scattering measurements of the O and Ni core levels collecting 2D diffraction patterns with 150° azimuth span. We extracted the modulation function $\chi(\theta, \phi) = (I(\theta, \phi) - I_0(\theta))/I_0(\theta)$ [where $I_0(\theta)$ is the average value of each azimuthal scan] for three Al $2p$ and two O $1s$ core level shifted components, corresponding all together to five nonequivalent Al and O species, with an overall angular span of about 22000°. Multiple-scattering simulations were performed using the EDAC code [21,22] running on a large scale calculation farm. The unit cell used in the simulations consisted of 721 atoms in the alumina film laying on six layers of $Ni_3Al(111)$ substrate, yielding additional 1608 atoms and a remarkable overall cell size of 2329 atoms. Photoelectron diffraction analyses of this size have not been performed before. In our structural optimization routine, each layer of atoms was moved rigidly, thus maintaining the intralayer positions of the DFT structure. This yielded a nine-dimensional space minimization problem, where the z position of the four (Al-O-Al-O) alumina layers, the z position of the two (Ni-Al) metal surface layers, the inner potential, the Debye temperature, and the height of the surface refraction plane were independently optimized in a recursive procedure, where the steepest descent method was used in order to minimize the R factor [18]. As a starting reference structure for the simulations, we used the atomic positions derived from the DFT model, where bulklike termination coordinates were assumed for the Ni_3Al atoms of the substrate [9]. Our assumption was that the DFT structure laid already in the same R factor hypersurface basin of the XPD absolute minimum. The uncertainties on the structural parameters were evaluated on the basis of the R factor variations according to [18].

Selected O $1s$ and Al $2p$ core level spectra are reported in Fig. 1, together with the best fit and the individual components obtained by fitting of the data using Doniach-Šùnjić envelopes [23] convoluted with a Gaussian.

The line shape parameters (asymmetry and Lorentzian width) and the peak positions, determined by analyzing spectra measured at different energies and emission angles, were subsequently kept fixed for the determination of the intensities angular dependence. Upon formation of a well-ordered alumina thin film, new components grow in the Al $2p$ core level spectrum with respect to the clean $Ni_3Al(111)$ surface (green). In addition to the bulk $2p_{3/2}$ component at 71.95 eV (black), three distinct features appear, accompanied by their spin orbit split replicas (not shown in the Figure). With reference to the bulk feature, a peak (+0.17 eV, gray, Al_s) grows, which is attributed to the surface Al atoms at the metal-oxide interface. Additionally, two progressively larger features appear at higher binding energies, which can be associated to the oxide interface layer in contact with the substrate (+1.14 eV, red, Al_i), and to the oxide termination (+2.67 eV, orange, Al_t), respectively.

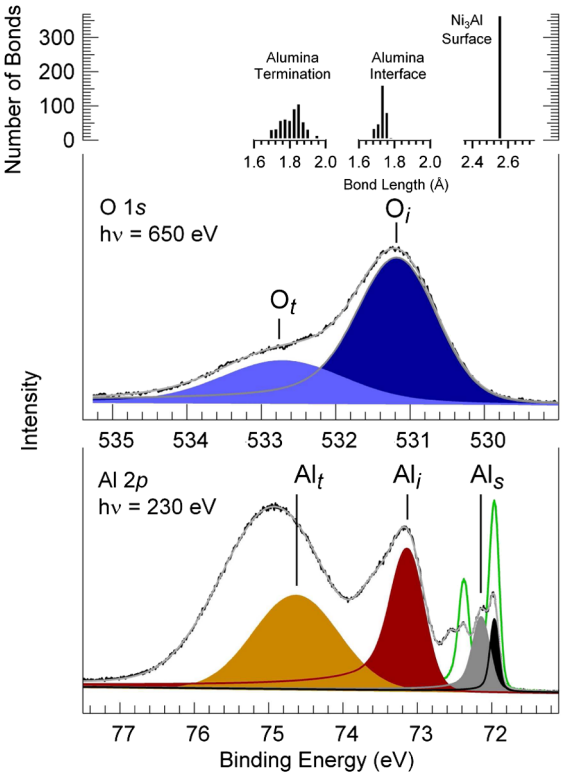

FIG. 1 (color online). Al $2p$ and O $1s$ core level spectra of the alumina/$Ni_3Al(111)$ film. Best fit and decomposition components are also shown (see text for details), together with the Al $2p$ spectrum corresponding to the clean surface (green). Intralayer Al-O and Al-Ni bond length distributions are depicted in the top panel.

The O $1s$ spectra present two components due to oxygen atoms at the metal-oxide interface (dark blue, 531.2 eV, O_i), and at the oxide terminal layer (blue, +1.58 eV, O_t), respectively. This assignment was initially proposed on the basis of previous spectroscopic information from a similar system [24], combined with the structural model details [9], and then validated by the analysis of the associated modulation functions.

An increase of the Gaussian width of the spectral components arising from O and Al atoms progressively closer to the oxide termination is observed. Even though it is well known that a spectral broadening is expected in the case of dielectric materials due to local charging effects, we additionally observe (Fig. 1, top panel) that there is a close correlation of the Gaussian width with the bond length distribution function [9], due to the variation of the Al-O and Al-Ni bond distances. Therefore, we associate this spectral behavior with the intralayer rippling of the oxide atomic planes, which is related to the variability of the nearest neighbor bond lengths. The structural optimization was performed using the full set of Al $2p$ and O $1s$ photo-

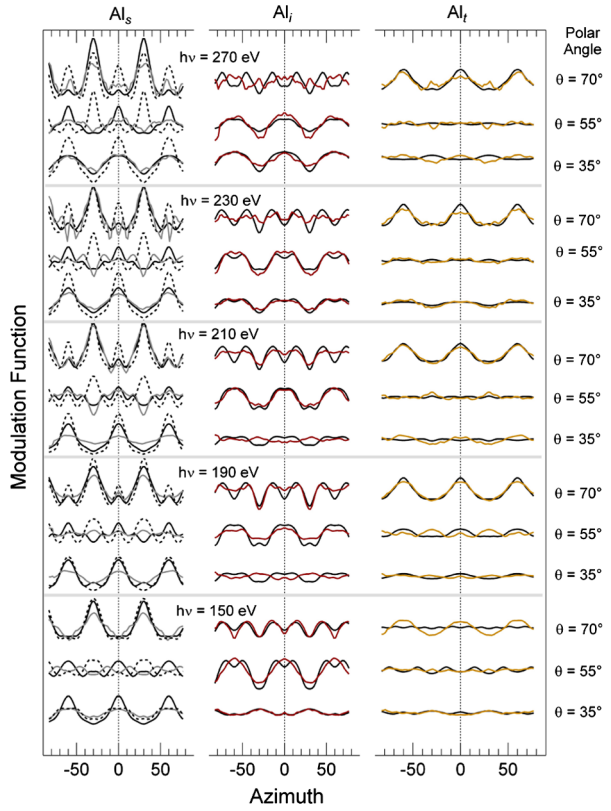

FIG. 2 (color online). Selected experimental (colored) and simulated (black) azimuthal modulation functions of the Al $2p_{3/2}$ components corresponding to surface, interface and termination Al atoms. Dotted black curves: simulated Al$_s$ modulation functions of the DFT structure without relaxation.

electron diffraction data, using the structure proposed in [9] as a starting point. Satisfactory agreement with the experimental modulation function was obtained only when full relaxation of the alumina and metal interlayer distances was allowed. A comparison of selected experimental and best R factor computed modulation functions for the Al $2p_{3/2}$ azimuthal scans is reported in Fig. 2. The O 1s data acquired in forward-scattering geometry provide complementary information about the relaxation within the oxide layers (Fig. 3).

On the basis of the full data set analysis, we obtain an R factor of 0.26 for the backscattering regime, corresponding to the structure depicted in Fig. 3. R factors of 0.08 and 0.17 are obtained for the terminal and interface oxygen components measured in forward scattering. If compared with the DFT proposed structure (R factor 0.51), we find a slightly compressed alumina film (Table I). The most remarkable outcome is, however, the ejection of the alloy first-layer Al$_s$ atoms towards the ultrathin oxide layer. In the case of the $Ni_3Al(111)$ [20] we already found a tendency for an outward relaxation (0.15 Å) with respect to the initially coplanar Ni atoms [20]. The geometrical arrangement significantly changes in the case of the alumina film: Al atoms located at the metal-oxide interface are lifted by 0.71 Å, yielding a first-to-second metal layer distance relaxation of +35% and a 30% contraction of the metal-oxide distance. The bottom layer of the oxide film mainly consists of an open array of Al hexagons, which are centered at the substrate Al positions. This allows accommodation of the metal surface Al atoms which lift and bind with both the bottom Al and O layers of the oxide film.

In order to obtain information about the interface Ni atoms, a different approach was adopted. Indeed, the O 1s and Al 2p XPD modulations in the backscattering regime resulted to be insensitive to the Ni atoms positions. In order to overcome this limit, we analyzed the ratio between the χ functions of the clean and ultrathin film covered surface, as obtained from the diffraction-induced angular modulation of the Ni 2p core level excited by the Al K_α radiation. The R factor analysis for different interface models allows us to conclude that the overall interface stoichiometry is maintained, while the Ni atoms of the metal surface are lifted in the same direction of the Al$_s$ neighbors by 0.35 Å.

Our findings provide the evidence for the formation of a new, low density, aluminum intermediate metallic layer at the metal-oxide interface, yielding as a consequence the formation of a pure Ni second layer, which is also lifted with respect to the bulklike termination. This provides the

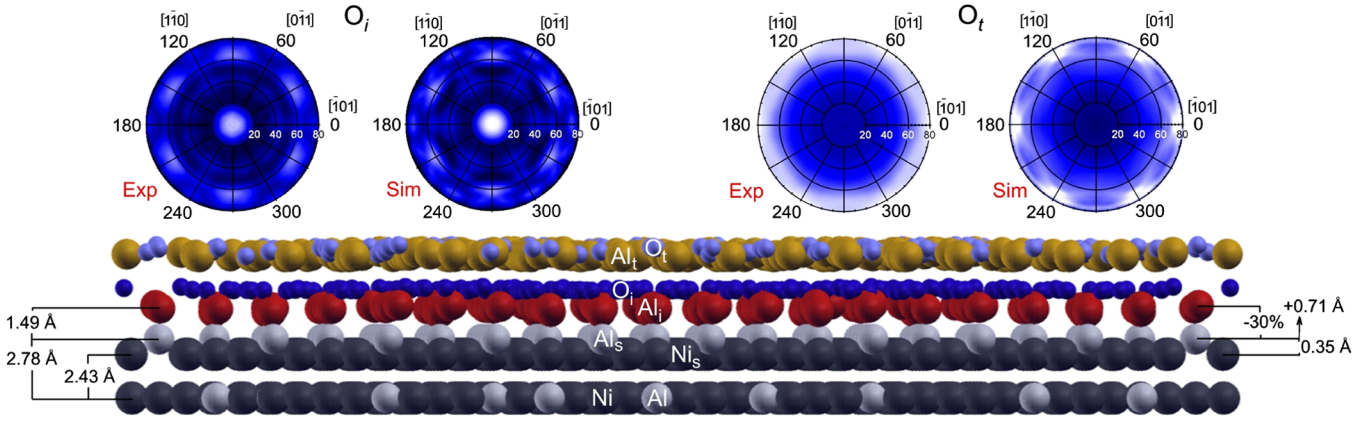

FIG. 3 (color online). O 1s experimental and simulated half-solid angle modulation function distributions in the forward-scattering regime, and the structural model of the relaxed oxide layers, including two Ni_3Al surface layers.

TABLE I. Average interlayer distances obtained from our data and from DFT calculations.

		This work	DFT [9]	Relax.
Ni_3Al	Al_s-II layer	2.78 ± 0.05 Å	2.07 Å	35%
	Ni_s-II layer	2.43 ± 0.10 Å	2.07 Å	17%
	Al_s-Ni_s	0.35 ± 0.10 Å	0.00 Å	
Oxide	Al_i-O_i	0.86 ± 0.05 Å	0.95 Å	−9%
	Al_t-O_t	0.24 ± 0.05 Å	0.44 Å	−45%
	Al_i-Al_t	2.50 ± 0.05 Å	2.73 Å	−8%
	O_i-O_t	1.88 ± 0.05 Å	2.22 Å	−15%

first experimental support to the interface model recently proposed on the basis of theoretical *ab initio* thermodynamics calculations, performed to investigate the properties of the alumina films grown on bimetallic alloy terminations [25]. Al accumulation at the NiAl-oxide interface was predicted for several oxide structures. In particular, in the proposed model the Al atoms in the first NiAl layer were lifted very close to the alumina film due to the interaction with the partially saturated oxygen bonds of the oxide. A few of them completely left the NiAl layer and migrated to the Al oxide second layer sites, yielding the complete buckling of the first NiAl layer and, consequently, the formation of a Ni-rich second layer, in analogy with our findings.

The formation of this new interface structure is crucial for the explanation of several properties of the aluminum oxide films. For example, the geometrical arrangement of the Al atoms at the interface is a key feature for the use of alumina coatings as protective layers [26]. Moreover, the generation of an electric dipole at the metal-oxide junction is strongly correlated with interface restructuring [27] and drives the changes in the Schottky barrier height. The latter is associated with a metal-oxide charge transfer which redefines the oxide electron properties [28]. In heterogeneous catalysis, access to these parameters would open the possibility to tune the band structure of the oxide film, and consequently to govern the electronic properties of the supported active metal clusters [29], which is a key issue in order to engineer new catalytic materials.

In conclusion, we have shown that large relaxation occurring at the interface between the ultrathin alumina film and the NiAl surface can be probed by using back- and forward-scattering photoelectron diffraction measurements. The observed atomic rearrangement, yielding the formation of separate metallic Al and Ni layers at the metal-oxide junction, is of fundamental importance for the determination of the transport properties of ultrathin films. More generally, we believe that the same approach, exploiting the elemental and chemical-state specificity of the technique, can be extended to the study of complex metal-oxide interfaces, which are expected to play a key role in the development of electronic devices with new superconductivity and magnetotransport properties.

We acknowledge financial support from Commissariato del Governo di Trieste (Fondo Trieste). We thank M. Peressi, S. Geremia, C. Barth, and Ph. Hofmann for fruitful discussions, M. Schmid for the DFT structure coordinates, and F. J. Garcia de Abajo for helpful discussions about EDAC. We are indebted to INFN-Sezione di Trieste for the access to the calculation cluster.

*alessandro.baraldi@elettra.trieste.it

[1] J. Heber, Nature (London) **459**, 28 (2009).
[2] A. Ohtomo and H. Y. Hwang, Nature (London) **427**, 423 (2004).
[3] A. Gozar *et al.*, Nature (London) **455**, 782 (2008).
[4] D. Goodman, J. Catal. **216**, 213 (2003).
[5] M. Bäumer and H.-J. Freund, Prog. Surf. Sci. **61**, 127 (1999).
[6] C. Freysoldt, P. Rinke, and M. Scheffler, Phys. Rev. Lett. **99**, 086101 (2007).
[7] L. Giordano *et al.*, Phys. Rev. Lett. **101**, 026102 (2008).
[8] P. Banerjee *et al.*, Nature Nanotech. **4**, 292 (2009).
[9] M. Schmid *et al.*, Phys. Rev. Lett. **99**, 196104 (2007).
[10] A. Stierle *et al.*, Science **303**, 1652 (2004).
[11] G. Kresse *et al.*, Science **308**, 1440 (2005).
[12] C. Becker *et al.*, J. Vac. Sci. Technol. A **16**, 1000 (1998).
[13] A. Rosenhahn, J. Schneider, C. Becker, and K. Wandelt, Appl. Surf. Sci. **142**, 169 (1999).
[14] S. G. Addepalli *et al.*, Surf. Sci. **442**, 385 (1999).
[15] S. Degen *et al.*, Surf. Sci. **576**, L57 (2005).
[16] G. Hamm *et al.*, Phys. Rev. Lett. **97**, 126106 (2006).
[17] S. Gritschneder, C. Becker, K. Wandel, and M. Reichling, J. Am. Chem. Soc. **129**, 4925 (2007).
[18] D. P. Woodruff, Surf. Sci. Rep. **62**, 1 (2007).
[19] A. Baraldi *et al.*, Surf. Sci. Rep. **49**, 169 (2003).
[20] E. Vesselli *et al.*, J. Phys. Condens. Matter **20**, 195223 (2008).
[21] F. J. Garcia de Abajo, M. A. Van Hove, and C. S. Fadley, Phys. Rev. B **63**, 075404 (2001).
[22] The code slightly differs from the original EDAC in order to correct a minor error related to the sign of the inner potential.
[23] S. Doniach and M. Šùnjić, J. Phys. C **3**, 285 (1970).
[24] A. Mulligan, V. Dhanak, and M. Kadodwala, Langmuir **21**, 8312 (2005).
[25] J. Feng, W. Zhang, W. Jiang, and H. Gu, Phys. Rev. Lett. **97**, 246102 (2006).
[26] L. Rivoaland, V. Amurice, M.-P. Bacos, and P. Marcus, Surf. Interface Anal. **34**, 400 (2002).
[27] R. T. Tung, Phys. Rev. B **64**, 205310 (2001).
[28] L. Giordano, F. Cinquini, and G. Pacchioni, Phys. Rev. B **73**, 045414 (2006).
[29] H.-J. Freund and G. Pacchioni, Chem. Soc. Rev. **37**, 2224 (2008).